Feedback Control of Oxygen Uptake During Treadmill Exercise

Kenneth J. Hunt, Bosun Ajayi, Henrik Gollee, and Lindsay Jamieson

***Abstract*—Regulation of exercise intensity is important for aerobic training and for exercise testing. Automatic control of oxygen uptake therefore has potential for use in exercise prescription and in tests to establish markers of cardiopulmonary status. The aim of this study was to investigate the feasibility of automatic feedback control of oxygen uptake during submaximal treadmill exercise. Six healthy male subjects aged 36.0 ± 12.2 years (mean ± standard deviation) ran on a computer-controlled treadmill while oxygen uptake was measured in real time using a breath-by-breath cardiopulmonary monitoring system. Linear dynamic models of oxygen-uptake response to changes in treadmill speed were obtained empirically using least squares optimization, and the models subjected to a cross-validation procedure. This resulted in selection of a first-order model with a time constant of 47 s. This model was used to design linear feedback controllers with a range of closed-loop bandwidth specifications. When implemented, each controller continuously monitored oxygen uptake and adjusted the commanded treadmill speed in real time in order to track a prespecified oxygen uptake profile. A series of closed-loop control tests illustrate that a single, fixed-parameter controller designed using a dynamic model from just one subject is robust enough to provide satisfactory control of a desired oxygen uptake profile for all subjects tested. Our results confirm the feasibility and robustness of automatic feedback control of oxygen uptake during treadmill exercise. Feedback regulation of exercise intensity via oxygen uptake may contribute to prescription of optimal training and testing programmes.**

***Index Terms*—Control engineering, exercise, feedback systems, identification, oxygen uptake, treadmill automation.**

I. Introduction

THE regulation of exercise intensity is important for aerobic training and for exercise testing. Automatic control of oxygen uptake therefore has the potential for use in exercise prescription and in tests to establish the key markers of cardiopulmonary status.

The main components of an aerobic training program are mode, frequency, duration, and intensity. Intensity is considered to be a very important variable for a number of reasons. It has been shown that high-intensity exercise elicits much greater improvements in aerobic power compared with low-intensity exercise [1]. Maintenance of aerobic fitness using high-intensity training is much more effective than low intensity [2]. However, high-intensity training is likely to result in a greater incidence of injury, subjective discomfort, and lower adherence to an exercise program. In addition, high-intensity training has the potential to promote health problems in subjects deemed to be at high risk, e.g., patients with cardiac disease [3], [4].

A number of methods are used to prescribe and monitor exercise intensity. These include oxygen uptake ($\dot{V}_{O_2}$), heart rate, ratings of perceived exertion (RPE), workrate, lactate threshold, and critical power. While heart rate can be monitored easily and cheaply, it is influenced by a number of factors including hydration status, time of day, and emotional state [5]. The accurate use of heart rate for training intensity depends on the determination of a representative maximum heart rate so that relative intensities can be established. It may be difficult and/or undesirable to attempt to find an individual's maximum heart rate. The use of heart rate may not be appropriate for some populations. For example, cardiac patients who are under beta blockade, or patients with a high-level spinal cord lesion, have a blunted heart rate response, which may not be representative of the metabolic cost of the exercise.

While RPE has been used as a substitute for $\dot{V}_{O_2}$ and heart rate, its use has limitations. A range of 12–15 for RPE has been shown to have a good relationship with a range of 58%–89% of $\dot{V}_{O_{2max}}$ [6], while a range of 11–14 has been linked to lactate threshold [7]. However, these ranges have been shown to have a wide interindividual variability, which limits the applicability of the general guidelines.

Exercise workrate can often be imposed with good accuracy, e.g., using the variable load on a cycle ergometer, or by varying the speed and gradient on a treadmill. However, some exercise tests require a specific $\dot{V}_{O_2}$ profile, such as an incremental exercise test for establishment of lactate threshold and maximal $\dot{V}_{O_2}$. Such tests are usually implemented through imposition of a specific workrate profile, under the assumption that $\dot{V}_{O_2}$ will then follow with the desired response.

Given that intensity is such an important variable for exercise training and testing, it is desirable to regulate intensity with great precision. The possible errors associated with heart rate and RPE may result in inappropriate intensities. One possible way of overcoming these difficulties is to regulate $\dot{V}_{O_2}$ during exercise. The precise regulation of a given $\dot{V}_{O_2}$ to correspond with a work rate at a given percentage of $\dot{V}_{O_{2max}}$, lactate threshold or critical power has the potential to be of benefit for exercise training and testing.

Regulating exercise intensity to a desired, sustainable level may contribute to the development of optimal training and testing programmes. The use of closed-loop feedback control would allow the instantaneous treadmill speed associated with the desired $\dot{V}_{O_2}$ to be obtained precisely and robustly, and would provide automatic, real time, adjustment of the speed to

Manuscript received January 30, 2007; revised May 22, 2007. Manuscript received in final form July 25, 2007. Recommended by Associate Editor A. Isaksson.

The authors are with the Centre for Rehabilitation Engineering, Department of Mechanical Engineering University of Glasgow, Glasgow G12 8QQ, U.K. (e-mail: k.hunt@mech.gla.ac.uk).

Digital Object Identifier 10.1109/TCST.2007.912116

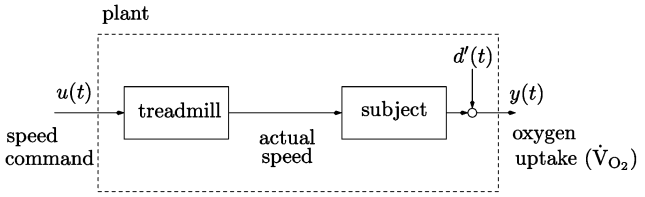

Fig. 1. Open-loop system consisting of treadmill, and subject running on the treadmill. The disturbance signal $d'(t)$ represents the effect of influences other than treadmill speed which affect the oxygen uptake.

maintain the desired $\dot{V}_{O_2}$ in the face of physiological adaptations or disturbances. This approach would therefore provide a self-regulating method of monitoring exercise intensity as it would not be necessary for the exerciser to monitor physiological responses to determine if the appropriate exercise intensity had been attained, or was being sustained.

Before it is possible to use this system within specific populations, it is first necessary to demonstrate that the conceptual approach for achieving a target $\dot{V}_{O_2}$ is technically feasible. To this end, we selected a subject group of healthy males, and the aim of this study was to investigate the feasibility of feedback control of $\dot{V}_{O_2}$ during submaximal treadmill exercise in this group. The proposed methodology encompasses: 1) estimation of the parameters of dynamic models of the response of $\dot{V}_{O_2}$ to changes in treadmill speed and cross validation of the estimated models; 2) analytical (model-based) design of feedback controller parameters to achieve a prespecified, nominal closed-loop $\dot{V}_{O_2}$ response profile. While point 1) has been widely studied in the literature, our proposal in point 2) for model-based design of feedback controllers for $\dot{V}_{O_2}$ is believed to be novel.

II. Methods

A. Structure of the Control Problem

The structure of the control problem under consideration is shown schematically in Fig. 1. The treadmill receives a speed command signal $u(t)$, which can be delivered manually through the treadmill's user interface panel or from a separate PC through a serial communication link. The speed command is received by an onboard speed controller which controls the treadmill motor. Thus, the actual speed of the treadmill lags the command signal to a degree dependent upon the speed controller's bandwidth and the treadmill motor performance. The speed of the treadmill acts as a forcing function for the subject running on the device, resulting ultimately in a measured oxygen uptake response ($\dot{V}_{O_2}$), denoted as the signal $y(t)$ in the figure.

In order to estimate a model of the overall dynamics of the response from the speed command $u(t)$ to oxygen uptake $y(t)$, a speed command signal of pseudorandom binary sequence (PRBS) format is imposed and the resulting oxygen uptake is measured while the system operates in the open-loop configuration shown in Fig. 1. These input–output data are then used to estimate and cross validate the parameters of dynamic transfer-function models linking u and y, as described in detail in the following (Section II-F). As indicated in Fig. 1, the given parts of the system that are to be controlled constitute the "plant."

The estimated dynamic model is then used in an analytical (model-based) feedback design procedure to determine the parameters of a feedback compensator for control of oxygen uptake (Section II-G). The structure of the proposed feedback system is shown in Fig. 2. Here, the dynamic feedback controller is denoted as C, and the aim is to ensure that the measured oxygen uptake follows a reference value in some prespecified manner. The controller operates on the oxygen uptake reference signal $r(t)$ and the oxygen uptake $y(t)$ [corrupted by a measurement noise signal $n(t)$ to give the measurement $y'(t)$], and continuously updates the treadmill speed command $u(t)$ in real time. Thus, the transient response of the closed-loop system depends on both the physiological response of the body to changes in workload and on the dynamics of the artificial controller component C. As described later, the controller dynamics are computed to ensure that a prespecified nominal closed-loop dynamic response is achieved.

Two quantitative performance measures are defined here for the evaluation of closed-loop controller performance. The first is the root mean square (RMS) tracking error, which gives a measure of the quality of reference tracking performance:

$$e(t)_{\mathrm{rms}} = \sqrt{\frac{1}{N}\sum_{t=1}^{N}(y^{\mathrm{nom}}(t) - y'(t))^2}. \tag{1}$$

Here, $y'(t)$ is the measured oxygen uptake and $y^{\mathrm{nom}}(t)$ is the nominal oxygen uptake response (i.e., the response with the simulated nominal model in the absence of disturbances and measurement noise). This performance criterion is defined over N sample instants, indexed by the discrete time variable t. The second measure is based upon changes in the controller output signal $u(t)$, defined as $\Delta u(t) = u(t) - u(t-1)$. The RMS value of this signal is

$$\Delta u(t)_{\mathrm{rms}} = \sqrt{\frac{1}{N-1}\sum_{t=2}^{N}(u(t) - u(t-1))^2}. \tag{2}$$

B. Gas Exchange Measurements and Data Processing

Oxygen uptake was measured in real time using a breath-by-breath cardiopulmonary monitoring system (MetaMax 3B, Cortex Biophysik GmbH, Leipzig, Germany). The system comprises a low dead-space mask, a gas analyzer for continuous measurement of respired O_2 concentration, and a turbine for measurement of airflow, from which gas volumes are derived. The O_2 analyzer in this system is an electrochemical cell which operates in the range 0%–35% O_2 with a response time of 100 ms. This response time is negligible with respect to the feedback control sample time of 10 s (see the following paragraph). Prior to each test, the volume transducer was calibrated using a 3-L syringe and the gas analyzers by two-point calibration with atmospheric air and a reference gas of certified concentration.

Feedback control requires real-time measurement of oxygen uptake ($\dot{V}_{O_2}$), synchronized to the discrete, regularly spaced sample instants at which the feedback loop operates. The sample

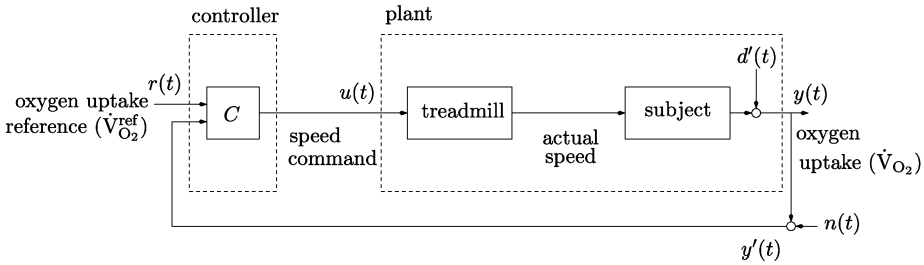

Fig. 2. Proposed feedback structure for closed-loop control of oxygen uptake. The signal $n(t)$ represents the effect of measurement noise.

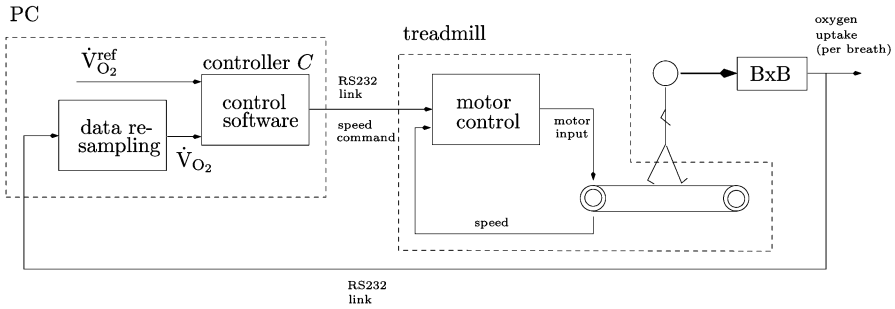

Fig. 3. Components of the treadmill, computer-based control system, and respiratory monitoring system (BxB signifies breath-by-breath measurement). Oxygen uptake measurements are obtained with each breath and passed to the computer where a resampling algorithm averages and realigns the data to the regular sample instants. The treadmill has a built-in speed control system.

time chosen for model estimation and feedback control was $T_s = 10$ s, which meets the general principle for discrete time feedback control design of having the order of ten samples over the chosen risetime of the closed-loop plant step response [8, p. 110] (closed-loop risetimes chosen here are between 100 and 200 s; see Section III-B).

The cardiorespiratory monitoring system was connected to a PC via an RS232 serial communication link to allow real-time measurement of oxygen uptake. Breath-by-breath measurement delivers an oxygen uptake value for every breath, distributed irregularly over time. At each sample instant, we therefore computed oxygen uptake as the mean of all discrete breath-by-breath values obtained during the preceding sample interval of 10 s. This introduces a time delay in the output measurement, but this is short in comparison to the open- and closed-loop risetimes, and is embedded within the experimental data used for identification.

C. Treadmill, Instrumentation, and Control

Experiments were carried out on a computer-controlled treadmill (T-track Gamma 300 model, Tunturi Oy, Ltd, Turku, Finland). The treadmill has a bidirectional RS232 serial link which was connected to a PC computer, thus allowing commanded treadmill speed to be set in real time, and real-time measurement of the actual speed to be monitored. Control software was implemented in Matlab/Simulink (The MathWorks, Inc., Natick, MA) running on the PC.

A schematic diagram showing the interface between real-time measurement and processing of oxygen uptake, feedback control software, and real-time speed commands sent to the treadmill is shown in Fig. 3.

TABLE I
SUBJECT CHARACTERISTICS

Subject	Age [yr]	Mass [kg]	Height [m]
A	31	61	1.73
B	41	76	1.85
C	28	74	1.75
D	34	70	1.73
E	24	92	1.85
F	58	76	1.76
mean $\pm$ sd	36.0 $\pm$ 12.2	74.8 $\pm$ 10.1	1.78 $\pm$ 0.06

D. Subjects

We present results here from tests conducted with six healthy male subjects, denoted A–F, who provided written, informed consent before inclusion in this study. Subject details are summarized in Table I. The subjects were recruited from within the research group (Centre for Rehabilitation Engineering, University of Glasgow, Glasgow, U.K.) and the lead author of this paper (K. J. Hunt) was one of the subjects. The study was approved by the Ethics Committee, Faculty of Biomedical and Life Sciences, University of Glasgow.

E. Study Design

All subjects were familiarized with the treadmill and cardiorespiratory monitoring equipment in advance of formal testing. The treadmill familiarization test allowed subjects to run at a self-selected speed, which they found to be sustainable. These tests were used to establish bounds on treadmill speed and oxygen uptake, which were enforced during subsequent identification and control tests.

One subject (A) participated in the open-loop treadmill tests designed to generate plant input–output data for model parameter estimation and validation. The treadmill speed command

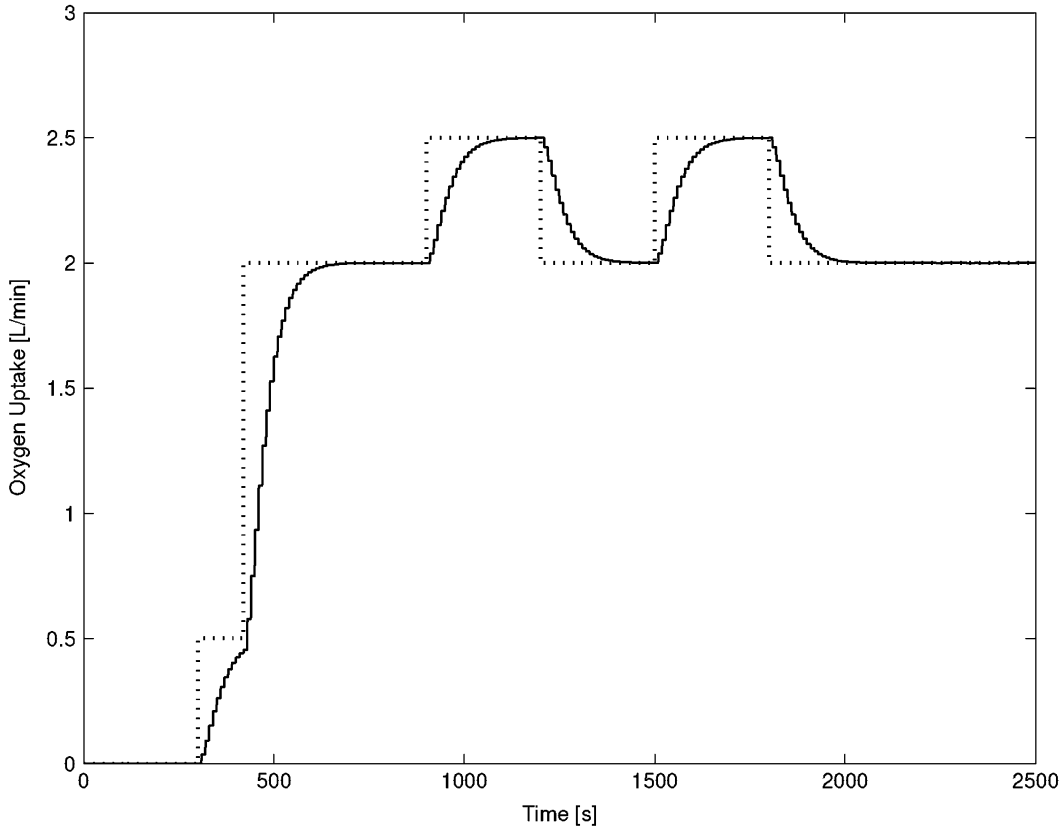

Fig. 4. Simulation of oxygen uptake reference signal [$r(t)$, dotted line], and nominal oxygen uptake response [$y(t)$, solid line]. Here, the nominal $\dot{V}_{O_2}$ response is based upon a closed-loop risetime specification of 100 s (i.e., t_m^r, or t_f^r, = 100 s; see the Appendix).

followed a PRBS profile as shown in Fig. 5 (lower plot), while oxygen uptake was recorded. The speed command is the plant input signal $u(t)$ and oxygen uptake is the plant output signal $y(t)$, as described in relation to Fig. 1. These data therefore describe the dynamic response of oxygen uptake to changes in the treadmill speed command signal. Following parameter estimation and validation as described in detail in Section II-F, one dynamic model was chosen to be used as the nominal plant model for feedback control design.

The nominal model was used to design three feedback controllers, which were each tested for real time $\dot{V}_{O_2}$ control with the "nominal" subject A, and with further subjects as detailed below. These controllers, denoted C1–C3, had different feedback and command-tracking bandwidths, by virtue of selection of the design parameters described in Section III-B. The controllers were evaluated using a square-wave profile for the commanded oxygen uptake response (reference signal $r(t)$ in the feedback structure of Fig. 2), as shown in the simulation results of Fig. 4. Fig. 4 also shows the prespecified, ideal output (oxygen uptake) response, illustrating that the square-wave command signal is "smoothed" by the dynamics of the closed-loop transfer function, in order that the demanded $\dot{V}_{O_2}$ profile is not subject to abrupt changes.

Following initial evaluation of the real-time performance of C1–C3, one controller (C3, designed using the model obtained with subject A) was selected for further real-time testing and evaluation with all subjects. This was done in order to test the robustness of the controller design; the controller was designed on the basis of open-loop response data from only one subject, and we wished to test its performance when applied to other subjects.

F. Model Structure, Parameter Estimation, and Model Validation

The open-loop plant is represented by a discrete time dynamic transfer-function model linking speed command $u(t)$ to oxygen uptake $y(t)$

$$\tilde{y}(t) = \frac{q^{-k}B(q^{-1})}{A(q^{-1})}\tilde{u}(t) + \frac{1}{A(q^{-1})}e(t). \tag{3}$$

This is known as an ARX model as it has an autoregressive part, $A\tilde{y}$, and an eXogenous input $\tilde{u}$. The signals $\tilde{u}$ and $\tilde{y}$ in (3) represent deviations from a steady-state operating point and are obtained from the raw plant input–output signals u, y by removal of constant offsets or trends in the data. The signal e is a notional error/disturbance signal. The orders of the polynomials A and B are denoted by na and nb, respectively, and estimates of the polynomial coefficients are obtained empirically using least squares optimization. Different model structures can be compared by computing the model "fit," which represents the percentage of output variation explained by the model (see the Appendix for details).

In the experiments reported here, test data obtained from one subject were used for model parameter estimation and validation using the procedures outlined previously and described in

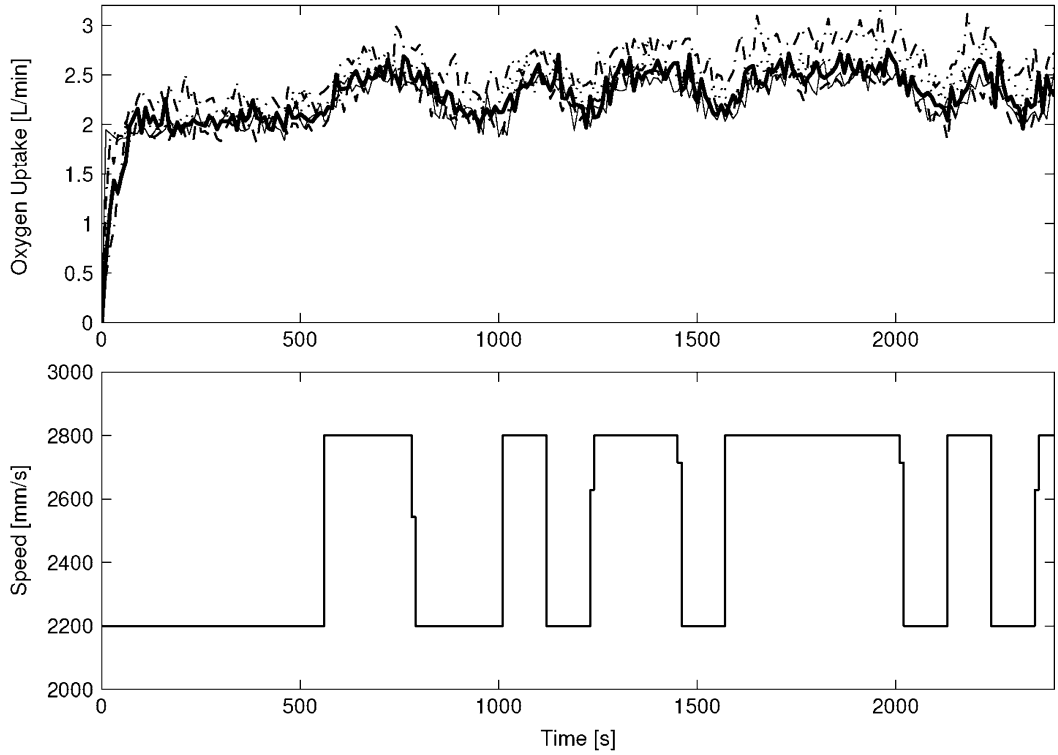

Fig. 5. Experimental input–output data used for parameter estimation and model validation (subject A). The lower plot shows the treadmill speed command (PRBS signal), which was applied in five separate tests, carried out on separate days. The upper plot shows the five oxygen uptake responses obtained.

detail elsewhere [9]. The subject repeated an open-loop treadmill test on five separate days, where the treadmill speed command was varied according to a prespecified PRBS profile and the subject's oxygen uptake was recorded. The format of the PRBS signal was chosen to excite relevant dynamic modes of the physical system, according to standard input design principles [9]. The PRBS speed signal is the plant input signal $u(t)$, while the oxygen uptake $\dot{V}_{O_2}$ is the measured plant output $y(t)$. Using the five data sets, model parameter estimation and validation was carried out in the following steps.

1) Each data set was used in turn to estimate the parameters of a range of model structures, i.e., estimates were obtained of the plant A, B polynomials with na chosen across the range $1 \ldots 4$, nb in the range $1, \ldots, 3$, and the discrete time delay ranged over $k = 1, \ldots, 4$.
2) The set of models obtained from estimation using a particular input–output data set was then validated by computing all model fit values [(15) in the Appendix] using the remaining four data sets.
3) The mean fit for each model structure across all validation data sets was then computed and the models compared.
4) One of the estimated models was chosen as the nominal plant model for feedback control design. The model was chosen on the basis of the model validation procedure described previously, and in consideration of the model complexity (i.e., the values of na, nb, and k).

G. Feedback Controller Design

The oxygen uptake controller C (Fig. 2) is a linear dynamic system whose parameters are obtained from an analytical (model-based) design procedure. The nominal dynamic model obtained from parameter estimation and validation (3), together with a specification of the desired speed of closed-loop response, is used in a feedback control design procedure to obtain the parameters of the controller. Full details of this procedure are given in the Appendix.

III. Results

A. Parameter Estimation and Model Cross Validation

Identification data with subject A are shown in Fig. 5. These five input–output data sets were used to estimate the parameters of ARX models of the form given by (3), for various combinations of the structural parameters na, nb, and k. The data sets were also used for cross validation of the estimated models according to the procedure outlined in Section II-F. A summary of the cross-validation results is presented in Table II.

From this analysis, the optimal delay is seen to be $k = 1$. Table II shows that, for models with $k = 1$, the fit improves as the order na of the estimated model increases, but that the magnitude of the improvement is not large. Since the order of the feedback controller increases with plant model order, it is desirable to reach an appropriate tradeoff between goodness of model fit and model order. In this case, since the mean fit for models with $k = 1$ does not increase significantly as the model order increases, the model with the fewest parameters, i.e., arx111, was selected for further investigation. This choice is supported by the fact that, on average, models with $na = 1$ have a higher fit value than models with $na > 1$ (rightmost column of Table II).

TABLE II
OVERALL CROSS-VALIDATION RESULTS: THE MODEL STRUCTURES INDICATED IN THE TABLE ARE INDEXED ACCORDING TO THE VALUES OF na [THE NUMBER OF A-POLYNOMIAL COEFFICIENTS; SEE (10)], $nb+1$ [THE NUMBER OF B-POLYNOMIAL COEFFICIENTS, SEE (11)], AND k (THE DISCRETE TIME DELAY), E.G., ARX112 IS AN ARX MODEL WITH $(na, nb+1, k) = (1, 1, 2)$. THE PARAMETERS OF EACH OF THE INDICATED MODEL STRUCTURES WERE ESTIMATED USING THE FIVE AVAILABLE DATA SETS IN TURN, THUS RESULTING IN THE AVAILABILITY OF FIVE MODELS FOR EACH STRUCTURE. EACH MODEL WAS THEN VALIDATED BY USING THE REMAINING FOUR DATA SETS (I.E., THOSE NOT USED FOR ESTIMATION OF THAT MODEL'S PARAMETERS) TO COMPUTE THE FIT VALUES ACCORDING TO (15), SO THAT THERE WAS A TOTAL OF 20 VALIDATION-FIT VALUES FOR EACH MODEL STRUCTURE. THE FIT VALUE SHOWN FOR EACH MODEL STRUCTURE IN THE TABLE REPRESENTS THE MEAN OF THE 20 VALIDATION VALUES FOR THAT STRUCTURE

Model	fit (%)	Model	fit (%)	Model	fit (%)	Model	fit (%)	mean
arx411	31.88	arx412	28.06	arx413	28.57	arx414	23.58	($na=4$): 28.02
arx311	31.20	arx312	29.01	arx313	27.58	arx314	22.52	($na=3$): 27.58
arx211	30.57	arx212	27.35	arx213	27.21	arx214	25.28	($na=2$): 27.60
arx111	29.11	arx112	29.76	arx113	28.66	arx114	27.81	($na=1$): 28.84
mean ($k=1$):	30.69	mean ($k=2$):	28.54	mean ($k=3$):	28.00	mean ($k=4$):	24.80	

TABLE III
MODEL VALIDATION RESULTS FOR MODEL STRUCTURE ARX111: FIVE ARX111 MODELS WERE ESTIMATED, USING EACH OF THE FIVE DATA SETS IN TURN AS INDICATED IN THE LEFT-HAND SIDE COLUMN. EACH MODEL WAS VALIDATED ON THE FOUR DATA SETS NOT USED FOR ESTIMATION, AND THE MEAN FIT ON THESE FOUR DATA SETS WAS COMPUTED, AS SHOWN IN THE RIGHT-HAND SIDE COLUMN. (NOTE THAT THE MEAN OF THE FIT VALUES IN THE RIGHT-HAND SIDE COLUMN IS EQUAL TO THE OVERALL MEAN CROSS VALIDATION FIT FOR ARX111 GIVEN IN TABLE II, I.E., 29.11%)

Estimation data set	arx111 fit (%)
5	34.83
2	34.13
1	28.38
3	25.76
4	22.45
mean	29.11

Table III shows the mean fit values for the five estimated arx111 models, ordered according to goodness-of-fit.

From this analysis, the arx111 model estimated from data set 5 (and validated on data sets 1–4) was selected as the nominal plant model for feedback control design and analysis. The parameters of this model [cf., (3)] are given by

$$\frac{q^{-k}\hat{B}(q^{-1})}{\hat{A}(q^{-1})} = \frac{b_0 q^{-1}}{1+a_1 q^{-1}} = \frac{0.2019\times 10^{-3} q^{-1}}{1-0.8097 q^{-1}}. \quad (4)$$

The steady-state gain of this model, which represents the increment in oxygen uptake resulting from an increment in treadmill speed, is 0.00106 L $\cdot$ min^{-1}/mm $\cdot$ s^{-1}, which indicates an increase of 106 mL $\cdot$ min^{-1} in oxygen uptake for an increase in speed of 100 mm $\cdot$ s^{-1}. The time constant of this model, i.e., the time taken for the output to increase from 0% to 63% of its final value in response to a step input, is 47.1 s.

B. Closed-Loop Control

The nominal model [see (4)] was used to design three feedback controllers, denoted C1, C2, and C3. The design parameters for these controllers are given in Table IV.

Controller C1, with a risetime of 100 s, was the first controller to be designed and was tested with subjects A, B, C, D, and E. A closed-loop control result with C1 for nominal subject A is shown in Fig. 6(a). This result indicated tight control of $\dot{V}_{O_2}$, but with a treadmill speed command signal, which was perceived by the subject to vary too rapidly (this conclusion held also for the other subjects tested with C1). The tightness of $\dot{V}_{O_2}$ tracking and the speed command signal variation are quantified in Table V.

TABLE IV
CONTROLLER DESIGN PARAMETERS (SEE THE APPENDIX FOR EXPLANATION)

Controller:	C1	C2	C3
loop risetime t_m^r (s)	100	200	200
observer risetime t_o^r (s)	30	30	30
pre-filter risetime t_f^r (s)	–	–	100

A second closed-loop controller (C2) was therefore designed with a slower desired closed-loop risetime of 200 s. C2 was tested with subjects A and B; the result with subject A is shown in Fig. 6(b). This result indicated a much smoother treadmill speed command signal, but slower $\dot{V}_{O_2}$ command tracking, as prescribed. The smoothness of the speed command signal is quantified in Table V: the RMS value of change in this signal Δu_{rms} is less than that for C1 by a factor of more than three.

Therefore, we designed a third controller C3 with design parameters chosen as a compromise between the fast $\dot{V}_{O_2}$ reference tracking qualities of C1 and the smooth treadmill speed command of C2. This was achieved by designing C3 with a reference prefilter (see the Appendix) with closed-loop tracking risetime specification of 100 s, but with an internal loop risetime of 200 s. The result with C3 and nominal subject A is shown in Fig. 6(c), and the quantitative performance for this controller is summarized in Table V. It is seen from the RMS tracking error that this controller tracks the reference less precisely than C1, but that the RMS command signal activity is less than that for C1 by a factor of more than two. That the command signal activity for C3 is approximately 50% greater than for C2 can be attributed to the faster risetime specification for C3; this therefore does not represent a performance degradation. Subjectively, subject A (and, subsequently, all other subjects) found treadmill speed variations with C3 to be acceptable.

This result was considered satisfactory and C3 was therefore tested with all remaining subjects, i.e., subjects B, C, D, E, and F: all of the closed-loop control results for C3 are shown in Fig. 7, and the RMS performance measures are summarized in Table VI.

The parameters of controller C3, obtained following the design procedure given in the Appendix using nominal model (4)

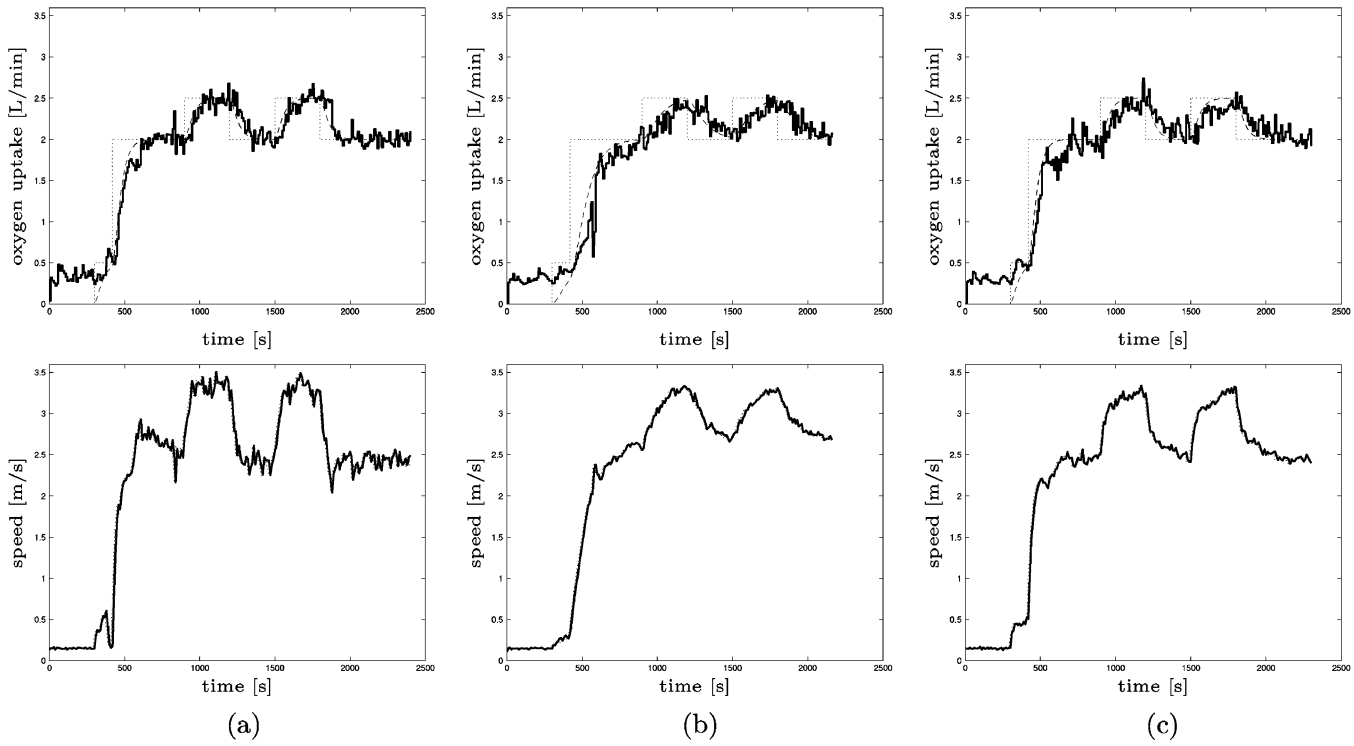

Fig. 6. Experimental results with subject A showing the effect of changing the controller parameters. Subject A is the nominal subject, i.e., the subject used for identification and control design. (a) Controller 1 has no prefilter. (b) Controller 2 has no prefilter and is slower than controller 1. (c) Controller 3 has a prefilter with risetime as in C1, but closed-loop poles as in C2 (see Table IV). The upper graphs in each part of this figure show oxygen uptake as follows (cf., Fig. 2): the measured closed-loop $\dot{V}_{\mathrm{O}_2}$ response $y'(t)$ (solid line); the nominal (i.e., simulated) $\dot{V}_{\mathrm{O}_2}$ response $y(t)$ (dashed line); the $\dot{V}_{\mathrm{O}_2}$ reference signal $r(t)$ (dotted line). The lower graphs in each subplot show the treadmill speed command signal $u(t)$ (dotted line) and the actual treadmill speed (solid line), in correspondence with the $\dot{V}_{\mathrm{O}_2}$ graphs in the upper row.

TABLE V
PERFORMANCE MEASURES FOR CONTROLLERS C1–C3 WITH SUBJECT A. e_{rms} IS THE RMS VALUE OF THE TRACKING ERROR $e(t)$ (1). Δu_{rms} IS THE RMS VALUE OF THE CHANGES IN TREADMILL SPEED COMMAND SIGNAL $u(t)$ [SEE (2)]. THESE VALUES ARE COMPUTED OVER THE TIME PERIOD FROM 800 TO 2000 S

Controller:	C1	C2	C3
e_{rms} [$\mathrm{L \cdot min^{-1}}$]	0.1300	0.1205	0.1520
Δu_{rms} [$\mathrm{mm \cdot s^{-1}}$]	130.30	42.40	60.04

and the design parameters for C3 shown in Table IV, are given by [cf., (16)]

$$R(q^{-1}) = 1 - 1.3087q^{-1} + 0.3087q^{-2} \tag{5}$$
$$S(q^{-1}) = 345.57 - 274.54q^{-1} \tag{6}$$
$$T(q^{-1}) = 108.30 - 37.270q^{-1} \tag{7}$$
$$F(q^{-1}) = \frac{3.4309 - 5.8480q^{-1} + 2.4921q^{-2}}{1 - 1.4526q^{-1} + 0.5276q^{-2}}. \tag{8}$$

IV. DISCUSSION

Model Properties: The cross-validation results in Table II illustrate that, according to the empirical least squares criterion (13), the optimal discrete time delay is $k = 1$, but that the difference in mean fit between models with $k = 1, 2$, and 3 is not large (less than 3%). Since k represents the integer number of sample periods within which the deadtime of the system is enclosed, the similarity in mean fit between models with $k = 1$–3 and the large decrease in mean fit between models with $k = 3$ and $k = 4$ suggest that the deadtime of oxygen uptake dynamics, which corresponds to the onset of phase I kinetics [10], is less than 30 s. This agrees with the range of 15–20 s reported previously [11]. Note that the short time delay introduced as a result of the method of $\dot{V}_{\mathrm{O}_2}$ sampling (Section II-B) is embedded within this empirical estimation of discrete time delay.

Table II shows that on average the best model order na is 1, but that there is little difference in mean fit for models in the range $na = 1$–4 (rightmost column of the table). This result supports the common assumption in the literature of a monoexponential function with time delay as a model of phase II oxygen uptake kinetics [10]. The 0%–63% risetime (i.e., the time constant of the equivalent monoexponential response model) of the estimated model with $k = 1$, $na = 1$ [see (4)] is 47.1 s, which is within the range of values expected for this population, given the magnitude of speed changes imposed with the PRBS forcing function.

On average, therefore, the cross-validation data support the choice of $k = 1$ and $na = 1$ as the structure of the model subsequently used for control design. Since the controller order, and therefore its complexity, increases with increasing k and na, it is advantageous to work with low-order, low-delay models for this purpose.

Feedback Control: The feedback control results illustrate that automatic feedback control of oxygen uptake during treadmill

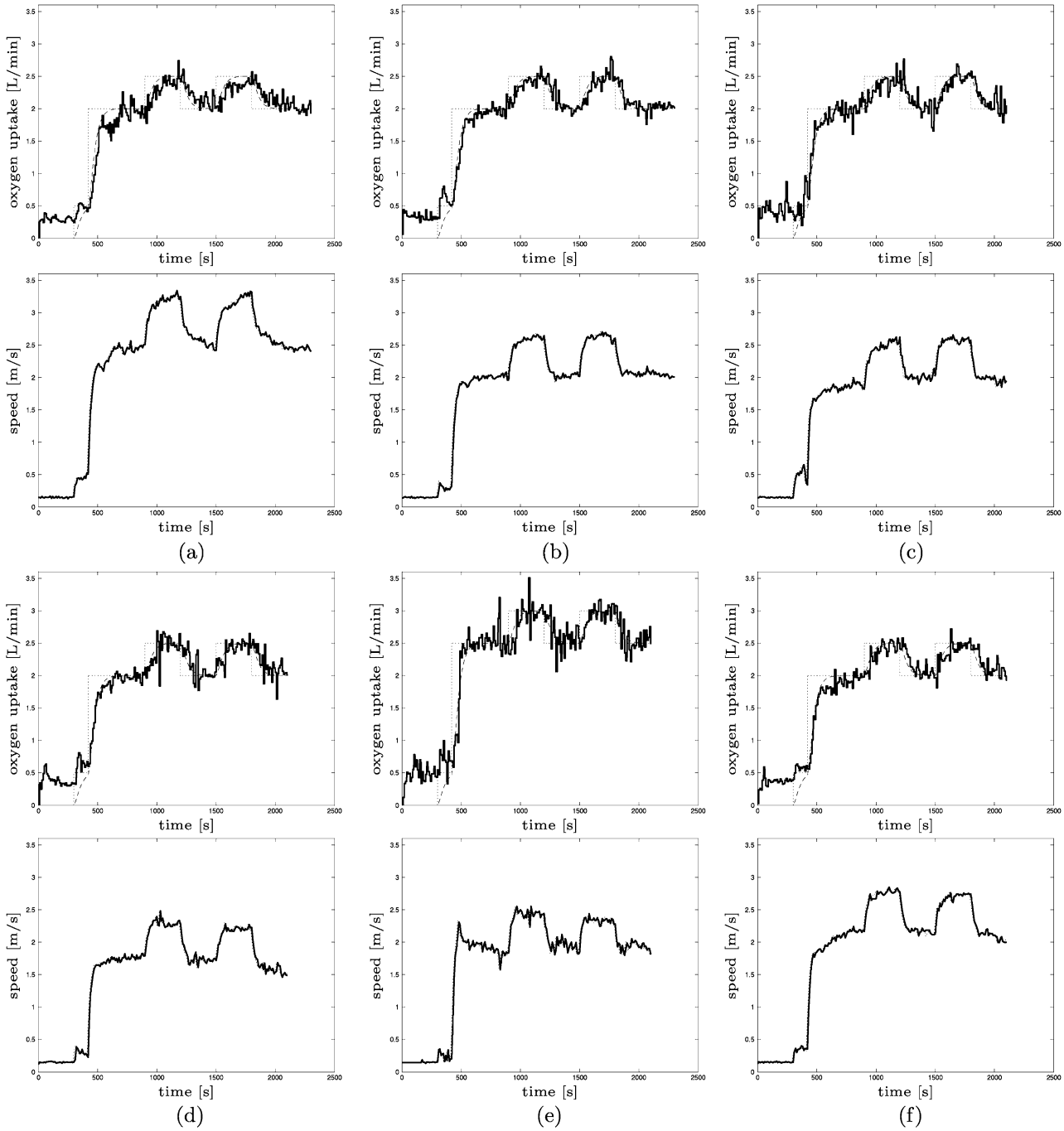

Fig. 7. Experimental results with controller 3 for subjects A–F. For a description of plot styles, see the caption of Fig. 6. (a) Subject A. (b) Subject B. (c) Subject C. (d) Subject D. (e) Subject E. (f) Subject F.

TABLE VI
PERFORMANCE MEASURES FOR CONTROLLER C3 WITH SUBJECTS A–F
($800\ \mathrm{s} < t < 2000\ \mathrm{s}$)

Subject:	A	B	C	D	E	F
e_{rms} $[\mathrm{L}\cdot\mathrm{min}^{-1}]$	0.1520	0.1174	0.1343	0.1508	0.1824	0.1252
Δu_{rms} $[\mathrm{mm}\cdot\mathrm{s}^{-1}]$	60.04	58.31	64.16	68.52	86.05	57.53

exercise, to achieve a prespecified $\dot{V}_{\mathrm{O}_2}$ profile, is feasible. This result is based upon empirical identification of oxygen uptake dynamics, together with an analytical design method which utilizes the estimated dynamic model. This approach allows the nominal closed-loop dynamics to be completely specified.

Specification of the nominal closed-loop system requires selection of three design polynomials, chosen here using familiar time-domain concepts of risetime and damping. These "tuning parameters" can be readily adjusted to achieve an appropriate tradeoff between disturbance rejection (as manifest in the tightness of steady-state regulation performance) and the smoothness of the control signal (treadmill speed command). This tradeoff is visible in comparing Fig. 6(a) with Fig. 6(b):

in comparison with controller 1, controller 2 has a smoother control signal, and a comparable regulation around the nominal $\dot{V}_{O_2}$ response. These differences are reflected in the objective performance measures reported in Table V.

By introducing the reference prefilter transfer function $F(q^{-1})$, which we have similarly designed here using rise-time and damping specifications, the reference signal tracking performance can be decoupled from the disturbance rejection characteristics of the closed loop. This is illustrated in Fig. 6(c), where controller 3 provides qualitatively similar regulation and control signal performance, but the nominal oxygen uptake reference tracking response is much faster than for controller 2 (100 versus 200 s).

The set of experiments shown in Fig. 7 illustrates that a single, fixed-parameter controller (designed using a model of subject A's $\dot{V}_{O_2}$ dynamics) is able to provide satisfactory control of oxygen uptake for all subjects tested, without the need for subject-specific model estimation and controller redesign. Qualitatively, the reference tracking and command signal performance for all subjects, with the exception of subject E, is similar. This observation is reflected in the measures presented in Table VI.

The performance measures for subject E appear to be appreciably poorer than the others. This may be attributable to the fact that this subject attained $\dot{V}_{O_2}$ levels of 2.0–2.5 L/min at a lower speed than other subjects, which was found not to be comfortable for running. For this reason, the $\dot{V}_{O_2}$ reference level was raised to 2.5–3.0 L/min for this subject, resulting in a running speed in the range 1800–2500 mm/s. The oxygen cost for this subject at this speed is clearly greater than for the other subjects, indicating poor running economy. Despite this clear variability in subject performance, it is notable that the controller maintains good tracking of the desired $\dot{V}_{O_2}$ profile.

These results indicate that a single controller may be robust for specific categories of subjects. This robustness property is due in part to the fundamental ability of feedback to handle plant uncertainty; in this case, steady-state tracking error is completely eliminated for all subjects through inclusion of integral action in the controller (this gives the controller infinite steady-state gain, so that the influence of constant disturbances and arbitrarily large steady-state plant model error are eliminated). In general, the ability to cope with unpredictable plant disturbances (up to the closed-loop bandwidth) and model error (resulting, for example, from intersubject variability, or from day-to-day physiological variation) are further basic properties of feedback which contribute to these results. The robustness of such a simple controller is also facilitated by the fundamental simplicity of the oxygen uptake dynamics: the estimated, nominal plant transfer function (4) shows that these are low order, open-loop stable, and minimum phase.

Exercise Physiology Implications: The results illustrate that the feedback control approach allows specific steady-state $\dot{V}_{O_2}$ levels to be automatically attained, and that accurate tracking of arbitrary $\dot{V}_{O_2}$ reference profiles corresponding to the prescription of various training-session exercise intensity profiles is also possible.

There is also relevance of the feedback method to exercise testing, for assessment of markers of cardiopulmonary status. In an incremental exercise test, for example, it is desirable to achieve linearity in the oxygen uptake time response, i.e., $\dot{V}_{O_2}$ should follow a linear ramp profile. This is usually achieved indirectly by imposing a linear increase in the exercise workrate. It is then assumed that the $\dot{V}_{O_2}$ response will follow as a linear function of time, but the actual linearity of $\dot{V}_{O_2}$ appears to be dependent upon the duration of the test [10, pp. 69–70], among other factors. A direct approach to achievement of linearity in the $\dot{V}_{O_2}$ response would be to use the feedback control approach proposed here and to impose a ramp-profile $\dot{V}_{O_2}$ reference signal. Any deviation of the actual $\dot{V}_{O_2}$ response from linearity would in principle be automatically corrected by the feedback, resulting in a nonlinear change in the forcing function instead (here, the treadmill speed command).

The generic methodology proposed here for design of $\dot{V}_{O_2}$ controllers can be translated straightforwardly to other ergometer systems, e.g., cycle ergometers. In this case, the exercise "forcing function" (generically, the controller output signal $u(t)$) would be the ergometer workrate, instead of treadmill speed.

This new approach to exercise prescription or testing based on feedback control of oxygen uptake requires the exerciser to be connected to a cardiorespiratory monitoring system for real-time measurement of oxygen uptake. However, to avoid the necessity for continuous breath-by-breath monitoring in situations where this is undesirable, and to approximately achieve the prescribed exercise intensity during exercise sessions, the following procedure can be used: 1) perform an open-loop test to determine appropriate markers of cardiopulmonary status [e.g., ventilatory lactate threshold (LT) or $\dot{V}_{O_{2\max}}$], so that the required exercise intensity can be determined (i.e., the $\dot{V}_{O_2}$ associated with specific percentages of LT or $\dot{V}_{O_{2\max}}$); 2) perform a single closed-loop test, in which the steady-state treadmill speeds associated with a finite number of steady-state $\dot{V}_{O_2}$ levels of interest (set via the $\dot{V}_{O_2}$ reference signal) are determined automatically; 3) in subsequent training sessions, implement a lookup table to determine the approximate treadmill speed required for a desired $\dot{V}_{O_2}$ [interpolating for values between the levels obtained in step 2)]—in these sessions, online measurement of $\dot{V}_{O_2}$ is not required; and 4) the lookup table can be recalibrated periodically by carrying out a closed-loop test, as in step 2), in order to adapt to changes in the exerciser's capacity.

V. Conclusion

Our results confirm the feasibility of a novel approach to automatic feedback control of oxygen uptake during treadmill exercise, and point to robustness of the design approach within the category of subjects tested.

The results show that feedback control is an appropriate method to regulate $\dot{V}_{O_2}$ in the selected population. The plant modeling and control design methodology proposed here is itself generic and can be widely applied, but further work is required to determine the extent to which other categories of subject can be successfully controlled with a single, fixed-parameter controller. If, for a given subject, an existing controller is not satisfactory, new plant identification tests and controller redesign would be required. It is anticipated that specific tuning of the feedback controller parameters may be required in other

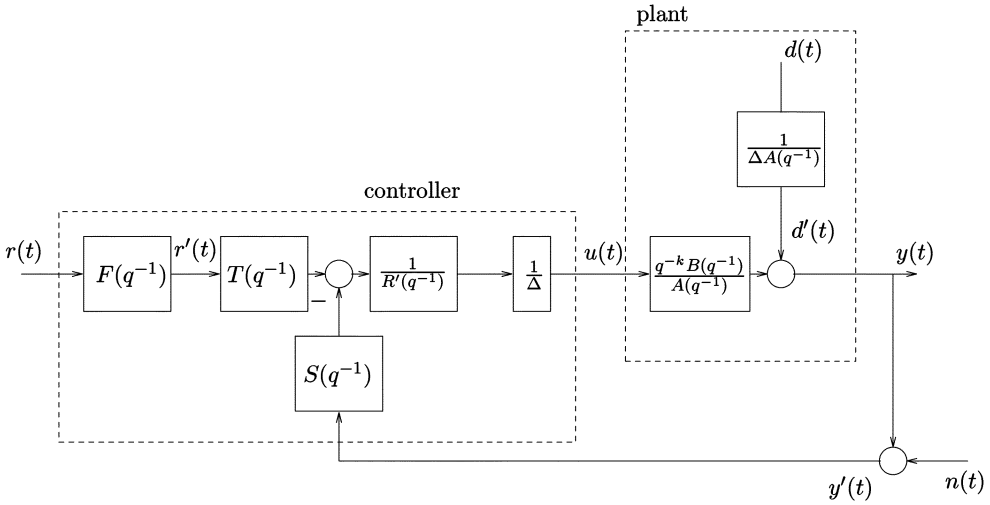

Fig. 8. Linear, discrete time representation of the feedback control loop.

subject groups with different aerobic fitness levels or in clinical populations.

The feedback regulation of oxygen uptake to a desired, sustainable level allows exercise intensity to be specified with great precision; this may contribute to the prescription of optimal training and testing programs.

APPENDIX

Plant Model and Parameter Estimation

The open-loop plant is represented by the discrete time dynamic model

$$y(t) = \frac{q^{-k}B(q^{-1})}{A(q^{-1})}u(t) + \frac{1}{\Delta(q^{-1})A(q^{-1})}d(t). \tag{9}$$

The integer $k \geq 1$ is a discrete input–output time delay, while A and B are polynomials in the delay operator q^{-1} [for any signal $x(t), q^{-1}x(t) = x(t-1)$] defined by

$$A(q^{-1}) = 1 + a_1 q^{-1} + \cdots + a_{na}q^{-na} \tag{10}$$

$$B(q^{-1}) = b_0 + b_1 q^{-1} + \cdots + b_{nb}q^{-nb}. \tag{11}$$

The net effect of disturbances is represented at the output by the signal d', modeled as the output of the filter $(1)/(\Delta(q^{-1})A(q^{-1}))$ driven by the signal $d(t)$. The polynomial Δ is defined as $\Delta = 1 - q^{-1}$. The output disturbance models the effect of stepwise-changing (piecewise constant) disturbances and offsets, which typically result from physiological and environmental factors.[1]

The plant polynomials A and B are estimated in an empirical identification procedure using least squares optimization. The procedure adopted here assumes an ARX model structure of the form given previously as (3), i.e.,

$$\tilde{y}(t) = \frac{q^{-k}B(q^{-1})}{A(q^{-1})}\tilde{u}(t) + \frac{1}{A(q^{-1})}e(t). \tag{12}$$

[1]In a stochastic framework, d is often taken as a compound or generalized Poisson process. See [12] for details.

The signals $\tilde{u}$ and $\tilde{y}$ in (12) are obtained from the raw plant input–output signals u, y following removal, as appropriate, of constant offsets or trends in the data. Here, constant offsets corresponding to the steady-state operating point of the plant are removed before identification. Denoting the input–output operating point as $(\bar{u}, \bar{y})$, we have $\tilde{y} = y - \bar{y}$ and $\tilde{u} = u - \bar{u}$. The signal e in (12) is an uncorrelated error/disturbance signal with appropriate stochastic definition. It is readily shown that, with these definitions, equations (9) and (12) are equivalent.

Parameter estimation uses a test input sequence $\tilde{u}(t)$ of length N and the corresponding, empirically measured output sequence $\tilde{y}(t)$. The least squares identification procedure delivers parameter estimates $\hat{A}, \hat{B}$ such that the following performance criterion is minimized:

$$J = \sum_{t=1}^{N}(\tilde{y}(t) - \hat{\tilde{y}}(t))^2 \tag{13}$$

where the predicted model output $\hat{\tilde{y}}$ is

$$\hat{\tilde{y}}(t) = \frac{q^{-k}\hat{B}(q^{-1})}{\hat{A}(q^{-1})}\tilde{u}(t). \tag{14}$$

Different model structures can be compared by computing the model "fit," which represents the percentage of output variation explained by the model, as defined by

$$\text{fit} = 100 \cdot \left(1 - \sqrt{\frac{\sum_{t=1}^{N}(\tilde{y}(t) - \hat{\tilde{y}}(t))^2}{\sum_{t=1}^{N}(\tilde{y}(t) - \bar{\tilde{y}})^2}}\right) \tag{15}$$

where $\bar{\tilde{y}}$ is the mean value of the measured output $\tilde{y}(t)$.

Feedback Controller Design Procedure

As shown in Fig. 2, the controller C operates on the $\dot{V}_{O_2}$ reference signal $r(t)$ and the $\dot{V}_{O_2}$ measurement signal $y'(t)$. The controller is described by the discrete time dynamic equation

$$u(t) = \frac{1}{R(q^{-1})}(F(q^{-1})T(q^{-1})r(t) - S(q^{-1})y'(t)) \tag{16}$$

where R, S, and T are polynomials in the delay operator q^{-1} and F is a transfer function. Integral action is included in the controller to ensure zero steady-state tracking error by constraining R as $R(q^{-1}) = \Delta(q^{-1})R'(q^{-1})$ (with $\Delta = 1 - q^{-1}$). With these definitions, and with the plant (9), the feedback system of Fig. 2 can be represented as the linear discrete time system shown in Fig. 8. The controller polynomials R, S, and T, together with the reference filter transfer function $F(q^{-1})$, are to be determined in the design procedure, which aims to achieve a prescribed nominal closed-loop response.

The closed-loop equation resulting from (9) and (16) is readily determined to be

$$y(t) = \frac{q^{-k}B(q^{-1})T(q^{-1})}{\rho(q^{-1})}F(q^{-1})r(t) + \frac{R'(q^{-1})}{\rho(q^{-1})}d(t) - \frac{q^{-k}B(q^{-1})S(q^{-1})}{\rho(q^{-1})}n(t). \quad (17)$$

Here, the closed-loop characteristic polynomial is denoted as ρ and is given by $\rho = AR + q^{-k}BS$, and it is this polynomial which determines the closed-loop response. We proceed by applying a standard pole assignment design method [8, Ch. 5], in which ρ is forced to match a prespecified set of closed-loop poles given by the product $A_m A_o$. Thus, the controller polynomials R and S are obtained as the solution of the linear polynomial equation

$$AR + q^{-k}BS = A_m A_o. \quad (18)$$

The polynomial $\rho = A_m A_o$ determines the response of the closed loop, but, by defining the controller polynomial T as a scaled version of A_o, it is only A_m, which determines the dynamics of the tracking response from r' to y. If desired, the closed-loop tracking response from r to y can be completely decoupled from the closed-loop poles by use of the tracking prefilter $F(q^{-1})$, which is a dynamic transfer function with a set of poles specified by a design polynomial $A_f(q^{-1})$.

The three design polynomials A_m, A_o, and A_f are chosen here using a time-domain approach to correspond to the poles of second-order transfer functions having a specified risetime and damping factor [13]. In this work, the damping factor was always selected as unity (critical damping). The three risetimes, chosen as detailed in the main text, are denoted t_m^r, t_o^r, and t_f^r, respectively. Full details of this analytical design procedure can be found in the literature [12], [8], [14].

ACKNOWLEDGMENT

The authors would like to thank Dr. S. Grant, formerly of the Faculty of Biomedical and Life Sciences, University of Glasgow, Glasgow, U.K., for his contribution to this paper.

REFERENCES

[1] H. A. Wenger and G. J. Bell, "The interactions of intensity, frequency and duration of exercise training in altering cardiorespiratory fitness," *Sports Med.*, vol. 3, pp. 346–356, 1986.

[2] R. C. Hickson, C. Foster, M. L. Pollock, T. M. Galassi, and S. Rich, "Reduced training intensities and loss of aerobic power, endurance and cardiac growth," *J. Appl. Physiol.*, vol. 58, pp. 492–499, 1985.

[3] "The recommended quantity and quality of exercise for developing and maintaining cardiorespiratory and muscular fitness in healthy adults," *Med. Sci. Sport Exerc.*, vol. 30, pp. 975–991, 1998, American College of Sports Medicine.

[4] J. S. Skinner, *General Principles of Exercise Prescription in Exercise Testing and Exercise Prescription for Special Cases. Theoretical Basis and Clinical Application*, 3rd ed. Baltimore, MD: Williams & Wilkins, 2005.

[5] W. D. McArdle, F. I. Katch, and V. L. Katch, *Essentials of Exercise Physiology*, 3rd ed. Baltimore, MD: Williams & Wilkins, 2001.

[6] T. G. Birk and C. A. Birk, "Use of perceived ratings of perceived exertion for exercise prescription," *Sports Med.*, vol. 15, pp. 496–502, 1987.

[7] A. Weltman, "The blood lactate response to exercise," in *Current Issues In Exercise Science*. Champaign, IL: Human Kinetics, 1995, Monograph Number 4.

[8] K. J. Åström and B. Wittenmark, *Computer Controlled Systems*, 3rd ed. New York: Prentice-Hall, 1997.

[9] L. Ljung, *System Identification: Theory for the User*, 2nd ed. New York: Prentice-Hall, 1999.

[10] K. Wasserman, J. E. Hansen, D. Y. Sue, R. Casaburi, and B. J. Whipp, *Principles of Exercise Testing and Interpretation*. Baltimore, MD: Williams & Wilkins, 1999.

[11] B. Whipp, S. Ward, L. Lamarra, J. Davis, and K. Wasserman, "Parameters of ventilatory and gas exchange dynamics during exercise," *J. Appl. Physiol.*, vol. 52, no. 6, pp. 1506–1513, 1982.

[12] K. J. Hunt, *Stochastic Optimal Control Theory with Application in Self-tuning Control*, ser. Lecture Notes in Control and Information Sciences. Berlin, Germany: Springer-Verlag, 1989, vol. 117.

[13] K. J. Hunt, M. Munih, N. Donaldson, and F. M. D. Barr, "Optimal control of ankle joint moment: Toward unsupported standing in paraplegia," *IEEE Trans. Autom. Control*, vol. 43, no. 6, pp. 819–832, Jun. 1998.

[14] V. Kučera, *Discrete Linear Control: The Polynomial Equation Approach*. Chichester, U.K.: Wiley, 1979.

Kenneth J. Hunt received the B.Sc. degree in electrical engineering (1984) and the Ph.D. degree in control theory (1987) from the University of Strathclyde, Glasgow, U.K., in 1984 and 1987, respectively. He was awarded a D.Sc. degree for work in rehabilitation engineering by the University of Glasgow, Glasgow, U.K., in 2005.

Currently, he is Wylie Professor of Mechanical Engineering and Director of the Centre for Rehabilitation Engineering, University of Glasgow. He is affiliated with the Queen Elizabeth National Spinal Injuries Unit at the Southern General Hospital in Glasgow. His research interests include the application of control engineering to problems in exercise physiology and spinal cord injury rehabilitation.

Bosun Ajayi received the B.S. degree (first class) in mechanical engineering from Obafemi Awolowo University, Ile-Ifethe, Nigeria, the MBA degree with emphasis in marketing and strategy from the University of Lagos, Lagos, Nigeria, the M.S. degree in engineering from the University of Bristol, Bristol, U.K., in 2000, and the Ph.D. degree with a focus on feedback systems for control of physiological variables during exercise from the Centre for Rehabilitation Engineering, Glasgow University, Glasgow, U.K., in 2005.

Currently, he works with a multinational oil company in Nigeria. He was a recipient of various international scholarships and awards which enabled him to study for his M.S. and Ph.D. degrees in the United Kingdom. His research interests include control systems applications.

Dr. Ajayi is a Chartered Mechanical Engineer in the United Kingdom (CEng, MIMechE) and a member of the American Society of Mechanical Engineers (ASME). He is also a Microsoft Certified Professional (MCP).

Henrik Gollee graduated from the Department of Electrical Engineering, Technical University Berlin, Berlin, Germany, in 1995 and received the Ph.D. degree in systems and control from the University of Glasgow, Glasgow, U.K., in 1998.

Currently, he is a Lecturer at the Department of Mechanical Engineering and Assistant Director of the Centre for Rehabilitation Engineering, Glasgow University. His research interests include the application of advanced control methods in assistive technology with the primary focus on applications in spinal cord injury rehabilitation.

Lindsay Jamieson received a first degree in physiology and sports science and the Ph.D. degree in novel methods of exercise testing during treadmill walking in incomplete spinal cord injury from the University of Glasgow, Glasgow, U.K., in 2003 and 2007, respectively.

Currently, she is a Research Assistant at the Centre for Rehabilitation Engineering, University of Glasgow. Her research interests are in the study of physiological responses to exercise in spinal cord injury, including body-weight-supported treadmill training and robotic-assisted treadmill gait.

Dr. Jamieson received the Alan Stirling Brown prize from the University of Glasgow in 2007 in recognition of her Ph.D. work.